Structure and Fluxional Behavior of (η^4-butadiene)Fe(CO)$_2$L (L = CO, PH$_3$, PMe$_3$) Complexes. A Density Functional Study

Òscar González-Blanco and Vicenç Branchadell*,†

Departament de Química, Universitat Autònoma de Barcelona, Edifici Cn, 08193 Bellaterra, Spain

Received October 22, 1996[⊗]

The structure and fluxional behavior of (η^4-butadiene)Fe(CO)$_2$L (L = CO, PH$_3$, PMe$_3$) complexes have been studied using density functional methods. For (butadiene)Fe(CO)$_3$, the geometry obtained is in excellent agreement with the gas-phase experimental data. The calculation of the harmonic vibrational frequencies has permitted the reassignment of several frequencies observed in the IR and Raman spectra. The computed Fe−butadiene binding energy is in all cases about 52 kcal mol^{-1}, in excellent agreement with the experimental data corresponding to the (butadiene)Fe(CO)$_3$ complex. The nature of the bonding has been analyzed in terms of steric and electronic interactions. The butadiene−Fe rotational barriers have been computed, and the origin of the barrier has been discussed.

Introduction

Acyclic (diene)Fe(CO)$_3$ complexes have many applications as organometallic intermediates in asymmetric synthesis.[1−3] The most simple complex, (butadiene)Fe(CO)$_3$, has been known for many years,[4] and its structure has been determined both in the solid state[5] and in the gas phase.[6,7] In this complex, butadiene is coordinated through its four carbon atoms in an *s-cis* conformation. The structure has been interpreted as a square pyramid in which the two double bonds of butadiene occupy two basal positions, while one of the carbonyl groups is in the apical position and the two remaining carbonyl ligands are in the other two basal positions. As a consequence, the complex presents C_s symmetry. The IR and Raman spectra of this complex have been studied,[8−10] with special emphasis in the 2000 cm^{-1} region.[9,10]

One of the characteristics of this kind of complex is its fluxional behavior.[11−15] The ^{13}C NMR spectra at variable temperatures show an exchange between apical and basal carbonyl ligands. The barrier for this process has been estimated to be about 10 kcal mol^{-1}.[13,16] The substitution of one of the CO ligands by a phosphine enhances the reactivity of the complex,[17,18] and the presence of this ligand modifies the fluxional behavior.[18]

(diene)Fe(CO)$_2$L complexes have also been the object of theoretical studies.[19−27] Most of these studies, which are based on the extended Hückel method, have analyzed the bonding between butadiene and Fe in terms of the interactions between the molecular orbitals of butadiene and of Fe(CO)$_3$.[22−25,27] The fluxional behavior of the (butadiene)Fe(CO)$_3$ complex has also been discussed, and the conformational barrier has been attributed to the diminution of overlap between the molecular orbitals of the fragments at the transition state of the process.[18,23,27] The same kind of analysis has also been done for the rotational barrier of η^4-(trimethylenemethane)Fe(CO)$_3$.[22] The fluxional behavior of this system has recently been studied using density functional methods.[28] This study has shown that steric factors play a major role in the origin of the barrier.

The purpose of this paper is the study of the structure and fluxional behavior of the complexes (diene)Fe(CO)$_2$L (L = CO, PH$_3$, PMe$_3$) using density functional methods. The molecular geometries of these complexes will be

† E-mail: vicenc@quanta.uab.es.

⊗ Abstract published in *Advance ACS Abstracts,* December 15, 1996.

(1) *Organometallics in Organic Synthesis: Aspects of a Modern Interdisciplinary Field*; de Mejiere, A., tom Dieck, H., Eds.; Springer-Verlag: Berlin, 1987.
(2) Grée, R. *Synthesis* **1989**, 341.
(3) Nakamura, A. *Bull. Chem. Soc. Jpn.* **1995**, *68*, 1515.
(4) Reihlen, H.; Gruhl, A.; von Hessling, G.; Pfrengle, O. *Justus Liebigs Ann. Chem.* **1930**, *482*, 161.
(5) Mills, O. S.; Robinson, G. *Acta Crystallogr.* **1963**, *16*, 758.
(6) Kukolich, S. G.; Roehrig, M. A.; Henderson, G. L.; Wallace, D. W.; Chen, Q.-Q. *J. Chem. Phys.* **1992**, *97*, 829.
(7) Kukolich, S. G.; Roehrig, M. A.; Wallace, D. W.; Henderson, G. L. *J. Am. Chem. Soc.* **1993**, *115*, 2021.
(8) Davidson, G. *Inorg. Chim. Acta* **1969**, *3*, 596.
(9) Duddell, D. A.; Kettle, S. F. A.; Kontnik-Matecka, B. T. *Spectrochim. Acta* **1972**, *28A*, 1571.
(10) Gang, J.; Pennington, M.; Russell, D. K.; Basterrechea, F. J.; Davies, P. B.; Hansford, G. M. *J. Opt. Soc. Am. B* **1994**, *11*, 184.
(11) Warren, J. D.; Clark, R. J. *Inorg. Chem.* **1970**, *9*, 373.
(12) Kruczynski, L.; Takats, J. *J. Am. Chem. Soc.* **1974**, *96*, 932.
(13) Kruczynski, L.; Takats, J. *Inorg. Chem.* **1976**, *15*, 3140.
(14) Turner, J. J.; Grevels, F.-W.; Howdle, S. M.; Jacke, J.; Haward, M. T.; Klotzbücher, W. E. *J. Am. Chem. Soc.* **1991**, *113*, 8347.
(15) Claire, K. S.; Howarth, O. W.; McCamley, A. *J. Chem. Soc., Dalton Trans.* **1994**, 2615.
(16) Bischofberger, P.; Hansen, H.-J. *Helv. Chim. Acta* **1982**, *65*, 721.
(17) Howell, J. A. S.; Squibb, A. D.; Goldschmidt, Z.; Gottlieb, H. E.; Almadhoun, A.; Goldberg, I. *Organometallics* **1990**, *9*, 80.
(18) Howell, J. A. S.; Bell, A. G.; Cunningham, D.; McArdle, P.; Albright, T. A.; Goldschmidt, Z.; Gottlieb, H. E.; Hezroni-Langerman, D. *Organometallics* **1993**, *12*, 2541.
(19) Connor, J. A.; Derrick, L. M. R.; Hall, M. B.; Hillier, I. H.; Guest, M. F.; Higginson, B. R.; Lloid, D. R. *Mol. Phys.* **1974**, *28*, 1193.
(20) Elian, M.; Hoffmann, R. *Inorg. Chem.* **1975**, *14*, 1058.
(21) Mingos, D. M. P. *J. Chem. Soc., Dalton Trans.* **1977**, 21.
(22) Albright, T. A.; Hofmann, P.; Hoffmann, R. *J. Am. Chem. Soc.* **1977**, *99*, 7546.
(23) Hoffmann, R.; Albright, T. A.; Thorn, D. L. *Pure Appl. Chem.* **1978**, *50*, 1.
(24) Albright, T. A. *Acc. Chem. Res.* **1982**, *15*, 149.
(25) Sautet, P.; Eisenstein, O.; Nicholas, K. M. *Organometallics* **1987**, *6*, 1845.
(26) Marynick, D. S.; Kirkpatrick, C. M. *J. Mol. Struct.* (*THEOCHEM*) **1988**, *169*, 245.
(27) Calhorda, M. J.; Vichi, E. J. S. *Organometallics* **1990**, *9*, 1060.
(28) Branchadell, V.; Deng, L.; Ziegler, T. *Organometallics* **1994**, *13*, 3115.

S0276-7333(96)00896-5 CCC: $14.00

optimized, and for the parent compound, the harmonic vibrational frequencies will be computed. We will analyze the Fe−butadiene interaction in terms of steric and orbital interaction effects and compute the Fe−butadiene binding energy. Finally, the transition state of the fluxional process will be determined and the origin of the energy barrier will be analyzed.

Computational Details

All the calculations have been done using the ADF program.[29] The molecular geometries have been optimized using the method developed by Versluis and Ziegler.[30] Harmonic vibrational frequencies have been computed by numerical differentiation of analytic gradients.[31,32]

Two different levels of calculation have been used in the geometry optimizations. In the most simple one, the local density approximation (LDA)[33] has been used, with the parametrization due to Vosko *et al.*[34] In the highest level of calculation the gradient corrections to the exchange and correlation potentials due to Becke[35] and Perdew,[36] respectively, have been used. All the reported energies have been computed including the gradient corrections. We will refer to them as BP/BP, when the geometry has been optimized at the same level of calculation, and BP/LDA, when LDA optimized geometries are used. The 1s shell of C and O and the 1s2s2p shells of Fe and P have been treated by the frozen core approximation.[37] For the representation of the valence shells of C, O, and P we have used an uncontracted double-ζ basis set of Slater orbitals (STO) augmented with a set of 3d polarization functions.[38] For H, we have also used a double-ζ basis set augmented with a set of 2p polarization functions,[38] and for Fe, we have used a triple-ζ basis set.[38] A set of auxiliary s, p, d, f, and g STO functions,[39] centered on all nuclei, has been used to fit the molecular density and represent the Coulomb and exchange-correlation potential in each SCF cycle. In the geometry optimization of the systems containing the PMe_3 ligand, the polarization functions of the C and H atoms have not been included. However, the energies have been recomputed by including these functions.

Results and Discussion

We will present in the first place the optimized geometries of the complexes. For (butadiene)$Fe(CO)_3$ we will also present the computed vibrational frequencies. In the second section, we will discuss the results corresponding to the Fe−butadiene binding energy and the analysis of the interaction between butadiene and the metal fragment. Finally, in the third section, we will study the fluxional behavior of these complexes and compute the activation parameters.

Geometry and Vibrational Frequencies. Figure 1 presents the optimized structure of the (butadiene)-$Fe(CO)_3$ complex. The most important optimized geometry parameters are presented in Table 1 along with the experimental data. The comparison with the gas-phase experimental results shows that both levels of calculation yield excellent results. For the metal−ligand bond lengths, LDA leads to values slightly lower than the experimental ones. The maximum error is 0.056 Å for the $Fe-C_1$ and $Fe-C_4$ bonds. On the other hand, BP leads to metal−ligand bond lengths closer to the experimental ones. The maximum error is in the $Fe-C_5$ bond length, which is overestimated with respect to the experimental value by 0.026 Å. Both levels of calculation reproduce the experimental ordering between the lengths of the bonds between Fe and the terminal and internal carbon atoms of butadiene. Regarding the C−C bond lengths of the butadiene moiety, there is a difference between both sets of experimental data. The experimental results in gas phase show that the C_2-C_3 bond, which would be a single bond in isolated butadiene, is longer than the C_1-C_2 and C_3-C_4 bonds, which would be double bonds in isolated butadiene. This ordering is reversed in the crystal. Both theoretical methods lead to the same ordering as the

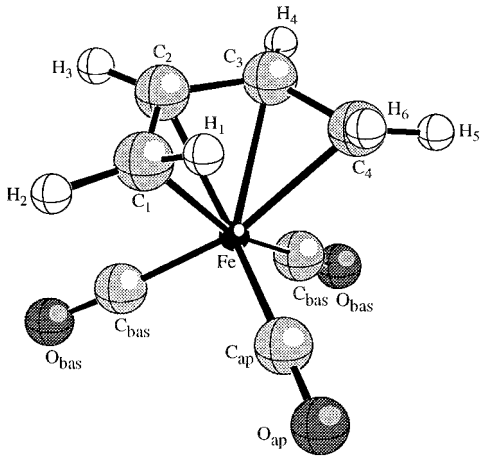

Figure 1. Structure of the (butadiene)$Fe(CO)_3$ complex.

Table 1. Selected Geometry Parameters of (butadiene)$Fe(CO)_3$

	calcd		expt	
param[a]	LDA	BP	X-ray[b]	microwave[c]
$Fe-C_{ap}$	1.739	1.796	1.74	1.770
$Fe-C_{bas}$	1.747	1.796	1.77	1.783
$Fe-C_1/Fe-C_4$	2.071	2.150	2.14	2.127
$Fe-C_2/Fe-C_3$	2.022	2.086	2.06	2.087
$C_{ap}-O_{ap}$	1.150	1.157	1.18	1.152
$C_{bas}-O_{bas}$	1.151	1.158	1.13	1.150
C_1-C_2/C_4-C_3	1.414	1.425	1.46	1.385
C_2-C_3	1.407	1.419	1.45	1.410
C_1-H_1/C_4-H_6	1.094	1.094		1.089
C_1-H_2/C_4-H_5	1.094	1.094		1.096
C_2-H_3/C_3-H_4	1.095	1.095		1.088
$C_{ap}-Fe-C_{bas}$	101.1	101.8	102	103.0
$C_{ap}-Fe-C_1/C_{ap}-Fe-C_4$	91.9	92.6		93.3
$C_{ap}-Fe-C_2/C_{ap}-Fe-C_3$	130.6	130.4		129.5
$C_{bas}-Fe-C_{bas}$	91.9	91.8	93	92.5
C_1-Fe-C_4	80.3	79.3	83	79.6
C_2-Fe-C_3	40.7	39.8		39.5
$Fe-C_{ap}-O_{ap}$	177.6	178.7	179	180.0[d]
$Fe-C_{bas}-O_{bas}$	178.6	178.9	178	180.0[d]
$H_1-C_1-H_2/H_6-C_4-H_5$	114.7	114.8		120.8
$H_1-C_1-C_2/H_6-C_4-C_3$	120.1	120.5		118.6
$H_2-C_1-C_2/H_5-C_4-C_3$	118.1	118.1		112.1
$H_3-C_2-C_1/H_4-C_3-C_4$	122.4	121.9		121.6
$H_3-C_2-C_3/H_4-C_3-C_2$	120.4	119.9		120.1
$C_1-C_2-C_3/C_4-C_3-C_2$	116.6	117.7		118.3

[a] See Figure 1. Bond lengths in angstroms and bond angles in degrees. [b] Reference 5. [c] Reference 7. [d] Fixed parameters.

(29) ADF, Department of Theoretical Chemistry, Vrije Universiteit, Amsterdam.
(30) Versluis, L.; Ziegler, T. *J. Chem. Phys.* **1988**, *88*, 322.
(31) Fan, L.; Ziegler, T. *J. Phys. Chem.* **1992**, *96*, 6937.
(32) Fan, L.; Ziegler, T. *J. Chem. Phys.* **1992**, *96*, 9005.
(33) Gunnarsson, O.; Lundquist, I. *Phys. Rev.* **1974**, *B10*, 1319.
(34) Vosko, S. H.; Wilk, L.; Nusair, M. *Can. J. Phys.* **1980**, *58*, 1200.
(35) Becke, A. D. *Phys. Rev. A* **1988**, *38*, 3098.
(36) Perdew, J. P. *Phys. Rev. B* **1986**, *33*, 8822.
(37) Baerends, E. J.; Ellis, D. E.; Ros, P. *Chem. Phys.* **1973**, *2*, 41.
(38) Vernooijs, P.; Snijders, G. J.; Baerends, E. J. *Slater Type Basis Functions for the Whole Periodic System*; Internal Report; Freie Universiteit Amsterdam: Amsterdam, 1981.
(39) Krijn, K.; Baerends, E. J. *Fit Functions in the HFS Methods*; Internal Report; Freie Universiteit Amsterdam: Amsterdam, 1984.

Table 2. Calculated Harmonic and Observed Fundamental Frequencies (in cm^{-1}) of (butadiene)Fe(CO)$_3$

A′			A″		
description	calcd	expt[a]	description	calcd	expt[a]
C−Fe−C bend	82		but−Fe torsion	75	
C−Fe−C bend	89	102[b]	C−Fe−C bend	96	102[b]
but−Fe−CO bend	131	135[c]	but−Fe−CO bend	119	135[c]
but tilt	370	363	but tilt	398	363
but−Fe stretch	410	379[d]	Fe−C−O bend	425	417[e]
C−C−C bend	476	453[d]	C−C−C−C torsion	481	464[d]
Fe−C−O bend	490	512	Fe−C−O bend	500	512
Fe−C stretch	531	493[e]	Fe−C stretch	542	567[f]
Fe−C stretch	552	567[f]	Fe−C−O bend	624	613
Fe−C−O bend	656	613	C−C−C bend	684	643[h]
Fe−C−O bend	679	669[g]	CH_2 twist	774	791[g]
CH_2 twist	794	774[h]	CH_2 wag	885	896
CH wag	873	926	CH wag	942	968[n]
CH_2 rock	909	926[i]	CH_2 rock	1033	1048[j]
CH_2 wag	933	954[j]	CH bend	1155	1174
C−C stretch	1059	1060[k]	CH_2 scissor	1336	1370
CH bend	1198	1205[l]	C═C stretch	1448	1439
CH_2 scissor	1429	1449	CO stretch	2031	1975 (2038[m])
C═C stretch	1474	1477	CH_2 stretch	3058	2929[o]
CO stretch	2045	1984 (2010[m])	CH stretch	3100	2950[p]
CO stretch	2102	2057 (2071[m])	CH_2 stretch	3152	3067
CH_2 stretch	3054	3012			
CH stretch	3112	3012			
CH_2 stretch	3150	3067			

[a] Reference 8. [b] Assigned to a but−Fe(CO)$_3$ bend. [c] Assigned to a C−Fe−C bend. [d] Assigned to an Fe−C stretch. [e] Assigned to a CCC bend. [f] Assigned to a Fe−C−O deformation. [g] Assigned to a CH wag. [h] Not assigned. [i] Assigned to a CH_2 wag. [j] Assigned to a CH_2 twist. [k] Assigned to a CH bend. [l] Assigned to a C−C stretch. [m] Reference 10. [n] Assigned to a CH_2 rock. [o] Assigned to a CH stretch. [p] Assigned to a CH_2 stretch.

crystal structure. The discrepancy between the theoretical results and the gas-phase experimental data mainly comes from an overestimation of the C_1-C_2 and C_4-C_3 bonds (0.029 Å at the LDA level and 0.040 Å at the BP level).[40] All experimental and theoretical results show that all C−C bonds in complexed butadiene have almost the same bond length, so that there is no difference between single and double bonds.

For the remaining geometry parameters the agreement between theory and the gas-phase experimental data is excellent. The only exceptions are the H−C−H and $H_2-C_1-C_2/H_5-C_4-C_3$ bond angles, in which there is a difference of about 6° between the experimental and the computed values. As a summary, we can conclude that both theoretical methods yield a geometry for the complex in very good agreement with the experimental gas-phase data. Moreover, LDA and BP calculations provide reasonably similar results.

The harmonic vibrational frequencies computed as the LDA level of calculation for the (butadiene)Fe(CO)$_3$ complex are presented in Table 2. All frequencies are real, thus confirming that the studied structure is an energy minimum. All frequencies have been assigned and compared with the experimental data reported by Davidson[8] for the whole vibrational spectrum and by Gang *et al.*[10] for the 2000 cm^{-1} region. For frequencies higher than 700 cm^{-1} the agreement between the computed and experimental values is excellent, with some exceptions. The most significant one regards the A′ CH_2 wagging and rocking modes and the A″ CH_2 wagging, rocking, and twisting, for which we have modified the assignments made by Davidson. Our assignments agree with the ordering obtained for *s-cis*-butadiene.[41] We have also reassigned the A′ C−C and CH bending frequencies. Complexation of butadiene produces a shift of the C═C and C−C stretching frequencies. In the first case, the computed values for *s-cis*-butadiene are 1643 cm^{-1} (A_1) and 1665 cm^{-1} (B_2), so that there is a shift of about −200 cm^{-1} upon complexation. The computed C−C stretching frequency for *s-cis*-butadiene is 871 cm^{-1}, so that the shift is +188 cm^{-1}. These shifts are consistent with the variation of the C−C bond lengths on complexation.

The assignment of the bands appearing at frequencies lower than 700 cm^{-1} is more problematic in the experiment,[8] since there is a strong mixing between the different modes. We have made our assignment by indicating the main contribution on each mode. We have reassigned several experimental frequencies in such a way that the difference between the computed and the experimental value is in all cases lower than 45 cm^{-1}. The mean deviation between computed and experimental frequencies is 31 cm^{-1} for the whole spectrum.

We have also studied the complexes (butadiene)Fe(CO)$_2$L (L = PH_3, PMe_3). For the PH_3 complex, we have considered two different structures that differ from each other in the position occupied by the phosphine ligand: apical or basal. At the BP/LDA level of calculation the first one is 1.0 kcal mol^{-1} more stable than the second one. For the (butadiene)Fe(CO)$_2$PMe$_3$ complex, we have only studied the structure in which the PMe_3 ligand is in the apical position. The most important geometry parameters of these complexes are presented in Table 3. If we compare the results corresponding to the PH_3 complexes with the ones corresponding to (butadiene)-Fe(CO)$_3$ (Table 1), we can observe that the substitution of a carbonyl group by a phosphine produces small changes in the geometry. For the PH_3-apical complex one can observe that the butadiene moiety is more distorted with respect to its equilibrium geometry[40] than

(40) The optimized C−C bond lengths for the isolated *s-cis*-butadiene at the LDA level are 1.332 and 1.451 Å for the C_1-C_2/C_3-C_4 bonds and for the C_2-C_3 bond, respectively.

(41) Guo, H.; Karplus, M. *J. Chem. Phys.* **1991**, *94*, 3679.

Table 3. Selected Geometry Parameters of (butadiene)Fe(CO)$_2$PR$_3$ Optimized at the LDA Level

param[a]	PH_3-apical	PH_3-basal[b]	PMe_3-apical
Fe−P	2.125	2.143	2.132
Fe−C_{ap}		1.728	
Fe−C_{bas}	1.732	1.728	1.726
Fe−C_1	2.078	2.074	2.071
Fe−C_2	2.015	2.029	2.017
Fe−C_3	2.015	2.025	2.017
Fe−C_4	2.078	2.059	2.071
C_{ap}−O_{ap}		1.156	
C_{bas}−O_{bas}	1.157	1.159	1.160
C_1−C_2	1.417	1.417	1.422
C_2−C_3	1.409	1.408	1.408
C_3−C_4	1.417	1.418	1.422
X_{ap}−Fe−X_{bas}[c,d]	101.3	101.5	97.1
X_{ap}−Fe−C_{bas}[c,d]	101.3	100.8	97.1
X_{ap}−Fe−C_1[c]	90.0	89.9	92.7
X_{ap}−Fe−C_2[c]	118.5	129.3	131.9
X_{ap}−Fe−C_3[c]	118.5	132.9	131.9
X_{ap}−Fe−C_4[c]	90.0	94.8	92.7
X_{bas}−Fe−C_{bas}[d]	92.2	89.9	92.5
C_1−Fe−C_4	80.3	80.5	80.2
C_2−Fe−C_3	40.9	40.7	40.9
Fe−C_{ap}−O_{ap}		177.3	
Fe−C_{bas}−O_{bas}	179.2	178.8	177.1

[a] See Figure 1. Bond lengths in angstroms and bond angles in degrees. [b] The PH_3 ligand is placed in the position closer to atoms C_1 and C_2. [c] X_{ap} represents the ligand in the apical position. [d] X_{bas} represents the ligand in the basal position.

in the (butadiene)Fe(CO)$_3$ complex. The Fe−C_2 and Fe−C_3 bond lengths are smaller, and the Fe−C_1 and Fe−C_4 ones are slightly larger. Regarding the Fe−CO distances, the values obtained for the PH_3 complex are smaller than the ones corresponding to (butadiene)Fe(CO)$_3$.

In the PH_3-basal complex there is no symmetry plane. The Fe−C_3 and Fe−C_4 bond lengths are slightly smaller than the Fe−C_2 and Fe−C_1 ones, respectively, due to the presence of the PH_3 ligand closer to the C_1 and C_2 atoms of butadiene.

If we compare the results obtained for the PMe_3 complex with the ones corresponding to the PH_3-apical complex, we can observe that they are very similar. The butadiene moiety is slightly more distorted with respect to its equilibrium geometry[40] and the difference between the terminal (C_1 and C_4) and internal (C_2 and C_3) Fe−C bond lengths decreases. The Fe−CO bond lengths are slightly smaller, while the Fe−P bond length is less than 0.01 Å larger.

Fe−Butadiene Binding Energies. Let us now present the results corresponding to the Fe−butadiene binding energies. For (butadiene)Fe(CO)$_3$ we have computed its binding energy relative to *s-trans*-butadiene and Fe(CO)$_3$. In this case we have assumed a C_{3v} structure[42] and a $^3A_2$ state, which has been shown to be the ground state.[43] The optimized structure is represented in Figure 2. We can observe that both the LDA and BP levels of calculation lead to similar geometry parameters. LDA underestimates the Fe−C bond length with respect to BP by 0.07 Å and the C−Fe−C and Fe−C−O bond angles by 5°. There are no experimental data regarding the geometry of Fe(CO)$_3$, and the only previous theoretical result corresponds to a partial geometry optimization at the MCPF level, which yields a value of 1.90 Å for the Fe−C bond length and a value of 1.18 Å for the C−O bond length.[43]

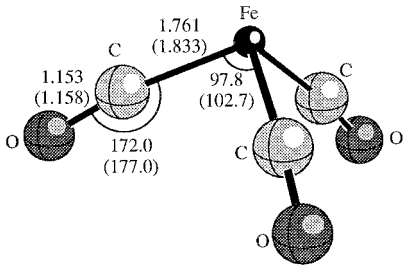

Figure 2. Geometry of the Fe(CO)$_3$ complex optimized at the LDA (BP) level. Bond lengths are in angstroms, and bond angles are in degrees.

For Fe(CO)$_2$PH$_3$ we have considered two different electronic states: $^1A'$ and $^3A''$. Our calculations show that the ground state is $^3A''$, while the $^1A'$ state is 11.6 kcal mol^{-1} higher in energy. According to these results, for Fe(CO)$_2$PMe$_3$ we have only considered the $^3A''$ state.

The Fe−butadiene binding energy in a (butadiene)Fe(CO)$_2$L complex can be decomposed into several contributions, according to the extended transition state method developed by Ziegler and Rauk.[44,45] According to this scheme, the binding energy (BE) can be expressed as follows:

$$BE = -(\Delta E_{prep} + \Delta E_{st} + \Delta E_{orb})$$

ΔE_{prep} is the preparation energy term, i.e., the energy necessary to convert the fragments from their ground-state equilibrium geometries to the geometry and electronic state involved in the complex formation. This term has a contribution from butadiene that will involve a *s-trans*/*s-cis* rearrangement and a geometry distortion and a contribution from Fe(CO)$_2$L. In this case we have considered that in the complex this fragment is in a singlet state,[46] so that its contribution to the preparation term will involve a triplet−singlet excitation and a geometry distortion. ΔE_{st} is the steric interaction term. This term represents the interaction energy between the two prepared fragments with the electron densities that each fragment would have in the absence of the other fragments. This term can be decomposed into an exchange repulsion or Pauli term (ΔE_{Pauli}) and an electrostatic term (ΔE_{elstat}). Finally, the orbital interaction term represents the stabilization produced when the electron density is allowed to relax. This term comes from the two-orbital two-electron stabilizing interactions between both fragments. The orbital term can be decomposed into a contribution arising from the butadiene → Fe electron donation, a contribution from the Fe → butadiene back-donation, and a synergic term that appears when both interactions are allowed. The computed binding energies of the (butadiene)Fe(CO)$_2$L complexes and its contributions are summarized in Table 4.

The basis set superposition error (BSSE) in the computed binding energies has been estimated using the counter poise (CP) method of Boys and Bernardi,[47,48] The CP correction is in all cases about 7 kcal mol^{-1}.

(42) Poliakoff, M. *J. Chem. Soc., Dalton Trans.* **1974**, 210.
(43) Barnes, L. A.; Rosi, M.; Bauschlicher, C. W. *J. Chem. Phys.* **1991**, *94*, 2031.
(44) Ziegler, T.; Rauk, A. *Theor. Chim. Acta* **1977**, *46*, 1.
(45) Ziegler, T.; Rauk, A. *Inorg. Chem* **1979**, *18*, 1558.
(46) We have assumed that the butadiene ligand is in the singlet electronic state arising for the same π orbital occupation as the one corresponding to its isolated ground state. For the Fe(CO)$_3$ fragment we have assumed a singlet state, with a $(15a')^2$ $(9a'')^0$ electronic configuration.[22−25,27]

Table 4. Decomposition[a] of the Butadiene−Fe Binding Energy[b] Computed for (butadiene)Fe(CO)₂L Complexes at the BP/LDA Level

		L = CO[c]	L = PH_3	L = PMe_3
ΔE_{prep}	$Fe(CO)_2L$	24.7 (24.9)	24.7	28.3
	butadiene	38.2 (35.4)	39.1	41.6
	tot.	62.9 (60.3)	63.8	70.0
ΔE_{st}	elstat	−166.2 (−138.7)	−171.9	−173.5
	Pauli	234.4 (185.3)	241.7	243.8
	tot.	68.2 (46.6)	69.7	70.3
ΔE_{orb}	but → Fe	−72.7 (−62.8)	−68.5	−67.7
	Fe → But	−100.4 (−85.0)	−107.1	−113.9
	synerg	−18.0 (−19.9)	−18.7	−18.9
	tot.	−191.1 (−167.7)	−194.4	−200.5
$\Delta E_{st} + \Delta E_{orb}$		−122.9 (−121.1)	−124.7	−130.2
BE		59.9 (60.8)	60.9	60.3
BE + BSSE[d]		52.4 (54.0)	53.9	52.6

[a] See text for definitions. [b] All contributions in kcal mol^{-1}. [c] Values in parentheses have been obtained at the BP/BP level. [d] Including the counter poise correction.

The Fe−butadiene binding energies have very similar values for the three complexes. For (butadiene)$Fe(CO)_3$ Brown *et al.*[49] have reported a bond enthalpy of 48 kcal/mol derived from microcalorimetric studies. Sunderlin *et al.*[50] have corrected this value to 56 ± 8 kcal mol^{-1}, by using more recent estimations of Fe−CO binding energies. In order to compare our results with this experimental data, we have computed the zero point vibrational energy from the LDA harmonic vibrational frequencies. The computed values of ΔH at 298.15 K and 1 atm are 50.4 (BP/LDA) and 52.0 (BP/BP) kcal mol^{-1}, in excellent agreement with the experiment data. The difference between the BP/LDA and BP results is 1.6 kcal mol^{-1}, so that the use of the LDA geometry involves an error less than 3% in the value of the binding energy. Both the steric energy and the orbital interaction energy are larger in absolute value for the LDA geometry. This is consistent with the values of the butadiene−Fe bond distances, which are smaller at the LDA level (see Figure 1 and Table 1). The sum of the steric and orbital energies is 1.8 larger in absolute value for the LDA geometry, but the larger preparation energy leads to a slightly smaller binding energy.

The value of the Fe−butadiene binding energy is the result of a steric repulsive contribution and an orbital stabilizing term. The larger contribution of this last term leads to a complex stable with respect to Fe−butadiene dissociation. The values of the contributions of the orbital energy term presented in Table 4 show that the orbital interaction contribution to the binding energy is mainly due to the back-donation from the occupied orbitals of Fe to the virtual orbitals of butadiene, with a smaller contribution due to the donation from butadiene to Fe. Most of these interactions are due to the HOMO and LUMO of the fragments, as schematically shown in **1** and **2**. Both interactions lead to an increase of the C_2-C_3 bond length and to a diminution of the C_1-C_2 and C_3-C_4 bond lengths.

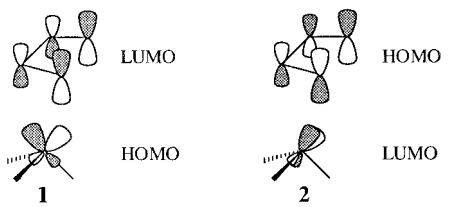

1 **2**

Let us now compare these results with the ones corresponding to the other two complexes. The preparation energy term slightly increases when going from L = CO to L = PH_3. The contribution of butadiene increases by 0.9 kcal mol^{-1}, while that of $Fe(CO)_2L$ does not change. For L = PMe_3, both contributions to the preparation energy increase, so that this term is 6.2 kcal mol^{-1} larger than for L = PH_3.

The steric energy term only slightly increases along the complexes. There is a parallel increase in the absolute values of the electrostatic and Pauli contributions that can be related to the change in the Fe−butadiene bond distances (see Tables 1 and 3). The fact that the steric energy term is about the same for the three complexes, while the preparation energy of the PMe_3 complex is noticeably larger than for the other complexes, shows that the steric repulsion produced by the methyl groups of PMe_3 is translated into a geometry distortion of the butadiene and $Fe(CO)_2L$ moieties.

The orbital interaction term increases in absolute value in the order CO < PH_3 < PMe_3. This is due to an increase of the Fe → butadiene back-donation contribution, which overtakes the diminution of the butadiene → Fe donation contribution. This fact is confirmed from the Mulliken population analysis of the complexes, which shows a net charge on the butadiene moiety of −0.018 au (CO), −0.115 au (PH_3), and −0.191 au (PMe_3). The variation of the donation and back-donation contributions to the orbital energy term shows that PMe_3 is a better σ-donor than PH_3 and CO, while it is a poorer π-acceptor.

The sum of the steric and orbital interaction terms is directly related to the bond enthalpy term defined by Martinho Simões and Beauchamp.[51] The variation of this term along the three complexes shows that the strength of the interaction increases in the order CO < PH_3 < PMe_3, in excellent agreement with the values of the Fe−butadiene bond lengths and the degree of geometry distortion of the butadiene moiety. When this term is added to the preparation energy, the resulting bond dissociation energies have almost the same value for all the complexes.

Rotational Barrier. The accepted mechanism for the exchange between apical and basal carbonyl ligands in the (butadiene)$Fe(CO)_3$ complex involves a turnstile rotation of the butadiene moiety relative to the $Fe(CO)_3$ moiety.[12,52] The transition state corresponding to this process would involve a structure in which one of the CO ligands would be eclipsed with the central C−C bond of butadiene. We have optimized the geometry of such a structure with the constraint of C_s symmetry, and we have obtained the geometry represented in Figure 3. This structure has an energy 9.6 kcal mol^{-1} higher than the minimum. This value of the rotational barrier is larger than the 7.2 kcal mol^{-1} reported by Albright *et al.*[22] The calculation of harmonic vibrational frequencies confirms that this structure is a stationary point on the potential energy hypersurface with an imaginary

(47) Boys, S. F.; Bernardi, F. *Mol. Phys.* **1970**, *19*, 553.
(48) Rosa, A.; Ehlers, A. W.; Baerends, E. J.; Snijders, J. G.; te Velde, G. *J. Phys. Chem.* **1996**, *100*, 5690.
(49) Brown, D. L. S.; Connor, J. A.; Leung, M. L.; Paz-Andrade, M. I.; Skinner, H. A. *J. Organomet. Chem.* **1976**, *110*, 79.
(50) Sunderlin, L. S.; Wang, D.; Squires, R. R. *J. Am. Chem. Soc.* **1992**, *114*, 2788.
(51) Martinho Simões, J. A.; Beauchamp, J. L. *Chem. Rev.* **1990**, *90*, 629.
(52) Ugi, I.; Marquarding, D.; Klusacek, H.; Gillespie, P. *Acc. Chem. Res.* **1971**, *4*, 288.

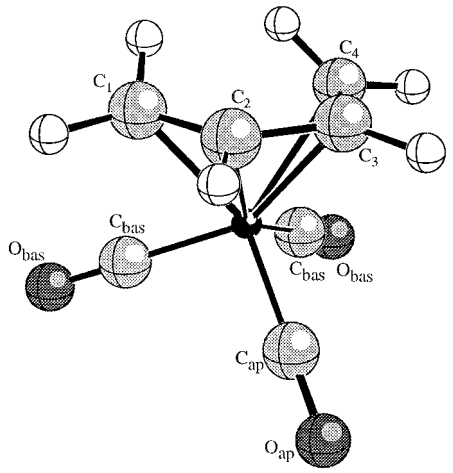

Figure 3. Geometry of the transition state corresponding to the butadiene−$Fe(CO)_3$ rotation in (butadiene)$Fe(CO)_3$. Bond lengths are in angstroms, and bond angles are in degrees.

Table 5. Selected Geometry Parameters of the Transition State of the Fluxional Process of (butadiene)$Fe(CO)_2L$ Optimized at the LDA Level

param[a]	L = CO	L = PH_3	L = PMe_3
Fe−X_{ap}[b]	1.747	2.135	2.141
Fe−C_{bas}	1.730	1.718	1.711
Fe−C_1/Fe−C_4	2.110	2.103	2.101
Fe−C_2/Fe−C_3	2.031	2.032	2.029
C_{ap}−O_{ap}	1.151		
C_{bas}−O_{bas}	1.154	1.160	1.163
C_1−C_2/C_3−C_4	1.406	1.408	1.412
C_2−C_3	1.419	1.420	1.419
X_{ap}−Fe−C_{bas}[b]	98.6	97.5	94.2
C_{bas}−Fe−C_{bas}	93.1	93.9	95.5
Fe−C_{ap}−O_{ap}	179.0		
Fe−C_{bas}−O_{bas}	179.5	179.6	177.1

[a] Bond lengths in angstroms and bond angles in degrees. [b] X_{ap} represents the ligand in the apical position.

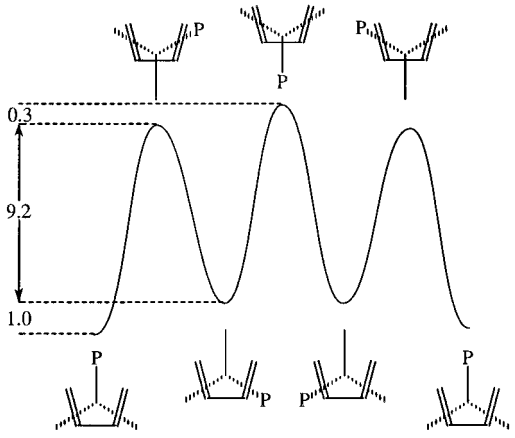

Figure 4. Schematic energy profile corresponding to the rotation around the butadiene−Fe axis in (butadiene)Fe-$(CO)_2PH_3$. Energy differences are in kcal mol^{-1}.

frequency, corresponding to the turnstile rotation. The most important geometry parameters corresponding to this transition state are presented in Table 5. For the PH_3 complex we have shown that there are two different energy minima. For this reason, there will be two kinds of transition states linking these minima. A schematic energy profile corresponding to the rotation of the butadiene moiety is presented in Figure 4. The highest transition state is the one in which the PH_3 ligand is in the apical position. This transition state has been located with the constraint of the C_s symmetry. The structure corresponding to the other transition state has been obtained by constraining one of the CO ligands to lie in a plane bisecting the butadiene moiety. For this reason, the energy barrier is somewhat overestimated, so that an unconstrained geometry search would not change the ordering between the energies of both transition structures. For the PMe_3 complex we have only considered the transition state in which the PMe_3 ligand is eclipsed with the central C−C bond of butadiene. The most important geometry parameters of these transition states are presented in Table 5.

Table 6. Decomposition[a] of the Rotational Barrier[b] Computed for the (butadiene)$Fe(CO)_2L$ Complexes at the BP/LDA Level

		L = CO	L = PH_3	L = PMe_3
$\Delta\Delta E_{prep}$	$Fe(CO)_2L$	1.4	3.2	3.8
	butadiene	−5.6	−5.7	−5.6
	tot.	−4.3	−2.5	−1.9
$\Delta\Delta E_{st}$	elstat	−4.4	−1.6	−3.8
	Pauli	14.2	9.9	14.3
	tot.	9.8	8.2	10.5
$\Delta\Delta E_{orb}$	but → Fe	−3.8	−3.7	−5.6
	Fe → But	5.6	6.7	6.6
	synerg	2.7	2.1	2.1
	tot.	4.4	5.2	+3.1
$\Delta\Delta E_{st} + \Delta\Delta E_{orb}$		14.2	13.4	13.6
$\Delta E^{\ddagger}$ [c]		9.9 (9.6)	10.8 (10.6)	11.7 (11.3)

[a] See text for definitions. [b] All contributions in kcal mol^{-1}. [c] Values corrected for the basis set superposition error in parentheses.

Table 6 presents the computed energy barriers corresponding to the fluxional process. We have analyzed them in terms of the same contributions used for the binding energies (see above). For (butadiene)$Fe(CO)_3$, this barrier can be compared with the experimentally observed CO exchange barriers,[13,16] For the PR_3 complexes we have considered the energy difference between the highest energy transition state and the lowest energy minimum. This energy barrier would correspond to the exchange of symmetry-equivalent CO ligands (see Figure 4), so that it would not be observable. However, the study of this energy difference will provide additional insight into the origin of the rotational barrier and will give us useful information for the prediction of barriers in related systems.

For (butadiene)$Fe(CO)_3$, Table 6 shows that the main contribution to the energy barrier arises from the steric energy term. This term mainly comes from the two-orbital four-electron repulsive interaction between the highest occupied orbitals of A″ symmetry of both fragments, **3**. The overlap between these two orbitals increases when going from the minimum to the transition state from 0.01 to 0.08

3

There is also a contribution of the orbital interaction term due to the Fe → butadiene donation. This term can be related to the diminution of overlap between the

HOMO of the Fe(CO)$_3$ moiety to the LUMO of butadiene, **1**. The value of this overlap decreases from 0.28 to 0.25 when going from the minimum to the transition state. On the other hand, the contribution due to the butadiene → Fe donation stabilizes the transition state with respect to the minimum. This fact would indicate that the interaction between the HOMO of butadiene and the LUMO of Fe(CO)$_3$, **2**, is more favorable at the transition state. This fact is not accompanied by an increase in the overlap between both orbitals. The computed overlap is 0.29 at the minimum and 0.28 at the transition state. As a result of these two effects, the contribution of the orbital interaction term to the energy barrier is less than half of the contribution of the steric energy, and it is compensated by the diminution of the preparation energy term due to the lower geometry distortion of butadiene at the transition state. These results show that the rotational barrier in (butadiene)Fe(CO)$_3$ is mainly due to the steric repulsion between butadiene and Fe(CO)$_3$ fragments at the transition state.

We have computed the activation enthalpy, entropy, and Gibbs energy at 298.15 K and 1 atm. The result obtained for $\Delta H^{\ddagger}$ is 9.9 kcal mol^{-1}, in excellent agreement with the experimental results obtained in solution by Kruczynski and Takats, 9.1 kcal mol^{-1},[13] and by Bischofberger and Hansen, 9.4 kcal mol^{-1}.[16] The computed activation entropy is +3.2 cal K^{-1} mol^{-1}. The experimental values are −4.6 cal K^{-1} mol^{-1} [13] and −1.7 cal K^{-1} mol^{-1}.[16] The computed value would correspond to a gas-phase process, while the experimental results correspond to processes in the presence of a polar solvent. The computed dipole moment of the energy minimum is 2.240 D, while for the transition state the value is 3.004 D. In both cases the direction of the dipole moment is that of the pseudo-C_3 axis of the Fe(CO)$_3$ moiety. Due to the larger dipole moment of the transition state, the contribution of solvation to the activation entropy would produce the change of sign from the gas-phase process. The computed value of the gas-phase Gibbs activation energy at 298.15 K and 1 atm is 8.9 kcal mol^{-1}, slightly lower than the experimental values in solution, 10.5 kcal mol^{-1} [13] and 9.9 kcal mol^{-1}.[16]

The substitution of one of the CO ligands by PH$_3$ produces a small increase in the value of the rotational barrier. This result can be compared with the increase from 9 to 12 kcal mol^{-1} reported by Calhorda and Vichi[27] for the rotational barrier in (benzylideneacetone)Fe(CO)$_2$L complexes. Table 6 shows that the increase in the rotational barrier is mainly due to the preparation energy of Fe(CO)$_2$PH$_3$ and to Fe → butadiene contribution to the orbital interaction term. The fact that the orbital interaction contribution to the barrier is larger for PH$_3$ than for CO would agree with the results obtained by Howell *et al.*[18] However, the barrier remains mainly due to the steric term. The contribution of this term to the barrier decreases when going from CO to PH$_3$. However, this fact does not mean that the steric requirements of CO are larger than those of PH$_3$. Steric repulsion between butadiene and Fe(CO)$_2$L can be minimized through geometry distortion of both fragments. The contribution of the Fe(CO)$_2$L fragment to $\Delta\Delta E_{prep}$ increases when going from CO to PH$_3$, while the contribution of butadiene remains almost constant. Regarding the results corresponding to the PMe$_3$ complex, we can observe that there is an important increase in the contribution of the steric term with respect to PH$_3$, while the increase in the contribution of the preparation term is smaller. In this case, the presence of the methyl groups makes the distortion of the Fe(CO)$_2$L moiety more difficult, so that the steric repulsion between this fragment and butadiene is larger.

Concluding Remarks

We have studied the complexes (butadiene)Fe(CO)$_2$L (L = CO, PH$_3$, PMe$_3$). We have optimized the geometries corresponding to the minimum energy conformations. For (butadiene)Fe(CO)$_3$ the comparison with the gas-phase experimental geometry shows an excellent agreement. The harmonic vibrational frequencies have been computed and compared with the experimental vibrational spectra. When several low-frequency vibrations are reassigned using the calculated values, the agreement between experimental and computed values is excellent. The Fe−butadiene binding energy has been computed for all the complexes, the values obtained being not dependent on the ligand L. For L = CO, the computed bond enthalpy is 52 kcal mol^{-1}, in very close agreement with the experimental estimate of 56 ± 8 kcal mol^{-1}.

The analysis of the bonding between butadiene and Fe shows that the main contribution to the stability of the complex comes from the Fe → butadiene back-donation. The contribution of this term increases in the order CO < PH$_3$ < PMe$_3$, following the ordering of σ-donor character of the ligand L.

The transition states corresponding to the conformational rearrangements in the complexes have been located. For (butadiene)Fe(CO)$_3$, the computed activation enthalpy is 9.9 kcal mol^{-1}, in excellent agreement with experimental data. The analysis of the energy barrier shows that it has an essentially steric origin. The value of the barrier increases when going from L = CO to L = PH$_3$, and L = PMe$_3$. This variation is due both to steric and orbital interactions.

Acknowledgment. This work has been financially supported by the DGICYT (Grant PB92-0621 and PB95-0640) and the CIRIT (Grant GRQ93-2079). O.G. gratefully acknowledges the Spanish Ministry of Education and Science for a doctoral fellowship. We also thank Prof. E. J. Baerends (Free University Amsterdam) for sending us a preprint of ref 48 prior to publication.

OM960896+